MedCrave
Step into the World of Research

Journal of Nanomedicine Research

# On Biodecorated Gold Nanoparticles Distributed within Tissues and Cells

**Abstract**

The size and surface charge of gold nanoparticles were reported to be key factors that determine their biological fate. The clearance half times of the biodecorated gold nanoparticles AuNPs from blood were reported to increase with decreasing the particle size. The particle elution time or the length of pathway is inversely proportional to the particle size. The positively charged nanoparticles were most toxic when compared with negatively charged particles and the neutral nanoparticles. Functional (ionic) surfactants (modifiers) have a pronounced effect on the distribution pattern not only by changing the circulation time in the bloodstream but also changing the nature of gold conjugates. The functional tissues present high activity to particle surface which favor their possible irreversible binding to biopolymers. The toxicity of the AuNPs is determined by their ability to irreversibly bind to key biomolecules (DNA and others) and change the functioning of cellular molecular processes.

**Keywords:** Noble metal nanoparticles; Preparation; Decoration; Penetration; Surface charge; Toxicity and biodistribution

Review Article

Volume 2 Issue 1 - 2015

**Ignac Capek***

*Slovak Academy of Sciences, Polymer Institute, Institute of Measurement Science, Bratislava and Faculty of Industrial Technologies, TnUni, Slovakia*

***Corresponding author:** Slovak Academy of Sciences, Polymer Institute, Institute of Measurement Science, Bratislava and Faculty of Industrial Technologies, TnUni, Slovakia, Tel: +421232294333; Fax: +421254775923; Email: ignac.capek@savba.sk

**Received:** November 14, 2014 | **Published:** February 19, 2015

**Abbreviations:** AAS: Atomic Adsorption Spectrometry; AuNP: Gold Nanoparticle; AuNR: Gold Nanorod; AuNS: Gold Nanoshell; BBB: Blood Brain Barrier; BSA: Bovine Serum Albumin; CA: Citric Acid; CALAA: Cys-Ala-Leu-Asn-Asn; CN: Cyano Groups; COOH: Carboxy Groups; $CTA^+$ ions: Cetyl Trimethyl Ammonium Cation; CTAB: Cetyl Trimethyl Ammonium Bromide; DNA: Deoxyribo Nucleic Acid; dsDNA: double-stranded DNA; Dx: Dextran; GSH: Glutathione, Tripeptide (Glutamic Acid, Cysteine and Glycine); hBMSC: Human Bone Marrow Stem Cell; $IC_{50}$: Inhibitory Concentration; ICP: Inductively Coupled Plasma; INAA: Instrumental Neutron Activation Analysis; NAA: Neutron Activation Analysis; LA: Lipoic Acid; Near-IR: Near Infra Red; $NH_2$: Amino Group; PAA: Polyacrylic Acid; PAH: Poly Allylamine Hydrochloride; PEG: Poly Ethylene Glycol; PEG-SH: Thiolated Poly Ethylene Glycol; PSS: Poly Styrene Sulfonate; PVP: Poly Vinyl Pyrrolidone; RA: Regression Analysis; RES: Reticulo Endothelial System; RNA: Ribo Nucleic Acid; SH: Thiol group; SPR: Surface Plasmon Resonance; ssDNA: Single-Stranded DNA; TEM: Transition Electron Microscopy; TNF: Tumor Necrosis Factor; XASX: Ray Absorption Spectroscopy

## Vocabulary

### Endocytosis

It is an energy-using process by which cells absorb molecules (such as proteins) by engulfing them. It is used by all cells of the body because most substances important to them are large polar molecules that cannot pass through the hydrophobic plasma or cell membrane. The opposite process is exocytosis.

### Lactate dehydrogenase (LDH)

It is of medical significance because it is found extensively in body tissues, such as blood cells and heart muscle. Because it is released during tissue damage, it is a marker of common injuries and disease.

### The MTT assay

It is a colorimetric assay for assessing cell viability.

### WSTs (water soluble tetrazolium salts)

These are a series of other water soluble dyes for MTT assays, developed to give different absorption spectra of the formed formazans. WST-1 is advantageous over MTT in that it is reduced outside cells. WST assays (1) can be read directly (unlike MTT that needs a solubilization step), give a more effective signal than MTT, and decrease toxicity to cells (unlike cell-permeable MTT, and its insoluble formazan that accumulate inside cells).

### Biotin

It also known as vitamin H or coenzyme R, is a water-soluble B-vitamin (vitamin B7). Biotin has an unusual structure, with two rings fused together via one of their sides. The two rings are ureido and thiophene moieties. Biotin is a heterocyclic, S-containing monocarboxylic acid.

### The mononuclear phagocyte system (MPS)

It is also called Reticuloendothelial System or Macrophage System is a part of the immune system that consists of the phagocytic cells located in reticular connective tissue. The cells are primarily monocytes and macrophages, and they accumulate in lymph nodes and the spleen. The Kupffer cells of the liver and tissue histiocytes are also part of the MPS.

## Introduction

Gold colloids are known for a long time even from ancient history. Colloidal gold was discovered in China as a "drug of longevity" since 2500 B.C. Indians have used colloidal gold (ash) in medicine for rejuvenation during the Vedic age. Somewhat

later gold colloids were adopted as a drug for vigor of youth and in the treatment of rheumatoid arthritis. Tremendous advances have been made in the synthesis of the noble metal nanoparticles and their applications over the past several decades. Currently, the plasmonic nanoparticles (microspheres, nanospheres, and ferrofluids) are applied in various fields of chemistry, physics, biology and medicine. Imaging, diagnostics, immunoassays, RNA and DNA purification, and gene cloning are interesting areas of nanomedicine. The colloids of noble metals, mainly gold and silver nanoparticles, are employed in a wide range of procedures and products including (nano)medicine, drug-delivery systems, biosensors, photothermal therapy, cosmetics, conductive ink, and lubricant oil. These applications are based on combining two principles:

a) Surface functionalization for providing the colloidal stability and biocompatibility of nanoparticles, the molecular recognition of conjugates, efficient endocytosis, etc.,

b) The excitation of plasmon resonances in the visible or near-IR region in order to obtain unique optical properties [1].

At nanometric scale, the physico-chemical and biological properties of materials differ fundamentally from their corresponding bulk counterpart. Nanoparticles have high surface-to-volume ratios when compared with large particles and are usually smaller than several hundred nanometers in size, comparable to large biological molecules, of a size about 100 to 10,000 times smaller than human cells. The range of studied gold nanoparticles covers more than two orders of magnitude from the minimal size of 1.0, 1.2 or 1.4 nm (atomic cluster $Au_{15}$, $Au_{35}$ or $Au_{55}$) [2] to the maximal size of 250 nm [3].

The noble metal nanoparticles can interact with biomolecules via S - bonds both on the surface and inside the body cells. These nanoparticles represent smart and promising candidates in the nanobiotechnology. Understanding the diffusion dynamics and receptor uptake mechanisms of nanoparticles and nanocarriers in various cells at single particle level is crucial for effective design of multifunctional nanostructures for imaging, targeting, and therapy. The nanoparticle size platforms that have been extensively explored for biomedical applications are summarized below. Among them biodistribution and toxicity of gold nanoparticles and their dependences on the particle size and shape, functionalization methods, doses, particle administration routes, and so on are discussed.

## Results and Discussion

### Preparation and properties

The preparation of noble metal nanoparticles has received considerable attention in recent decades because nanoparticles possess unconventional physical and chemical properties. These nanomaterials exhibit novel material properties which largely differ from the bulk materials due to these small sizes and new surface properties. For example, small and subnanoparticles of gold and silver can fluorescence, that is, absorb and emit light. Gold nanoparticlesare synthesized by the reduction of an aurate salt with reducing agents, such as sodium borohydride, thiocyanate, phosphorus, citrate and ascorbate in aqueoussolutions with or without surfactant. The synthesized gold nanoparticles are of nanometer size, with colors varying from yellow-orange to red-purple to blue-green. Bare (sub) nanoparticles usually during preparation or aging agglomerate tomicroparticles. The surface modification, however, improves their stability and biocompatibility. They can be modified with compounds carrying functional groups, such as cyano (-CN), thiol (-SH), carboxy (COOH) and amino (-$NH_2$) groups, known for their high affinity for gold (Figure 1). Additives having these functional groups can be used as capping agents for gold nanoparticles [4,5].

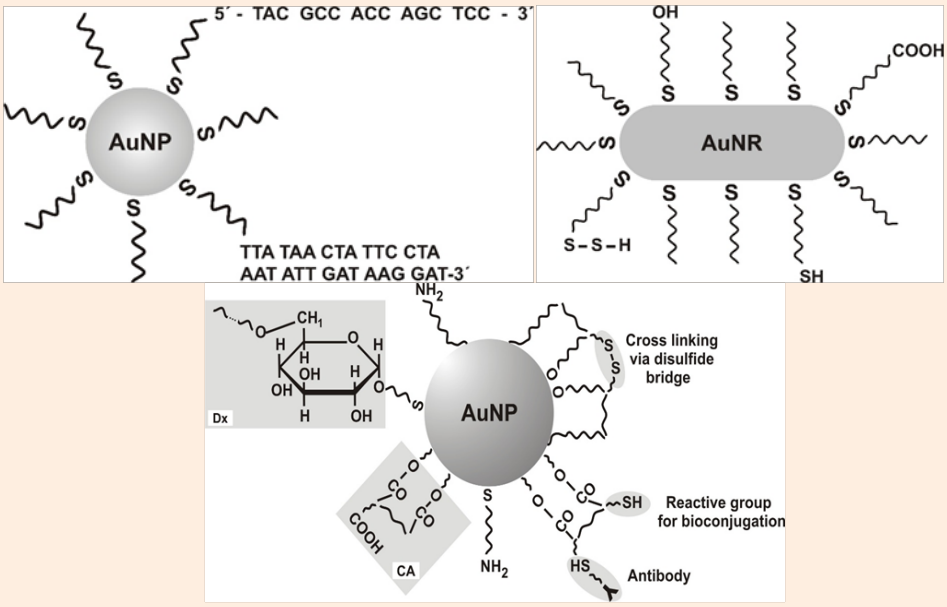


**Figure 1:** Schematics of gold nanoparticle (sphere (AuNP) and rod (AuNR)) modification-adsorption and chemisorption of ligands on the particle surface.

a) Top left panel: AuNP modified with ssDNA and dsDNA
b) Top wright panel: AuNR modified with alkyl thiols
c) Bottom panel: AuNP modified with dextran (Dx), citric acid (CA), 2,3-dimercaptosuccinic acid and other capping agents.

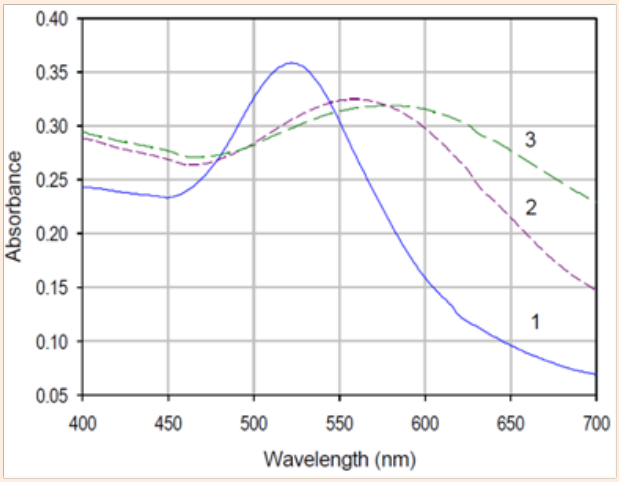


**Figure 2:** UV-Visible spectrum of
1. Gold nanoparticles (AuNP)
2. Glutathione capped AuNP and
3. Lipoic acid (LA) capped AuNP.

The reduction of $HAuCl_4$ by sodium citrate as a reducing agent leads to gold nanoparticles covered by a negative-charge layer arising from the residual negative citrate ions. This charge layer can be compressed or expanded depending on the total ionic concentration of the surrounding solution [6]. The functionalized (stable) gold nanoparticles are relatively monodisperse, which is confirmed by a single peak in the absorbance spectra (Figure 2) with the $\lambda_{max}$ at around 530 nm. The mean hydrodynamic size of the AuNP is in the range of 20-30 nm and after coupling (modified) to glutathione (GSH, tripeptide (glutamic acid, cysteine and glycine)) the approximate size was ca. 50 nm. As shown in Figure 2, the peak is shifted towards the higher wavelength after capping with glutathione (GSH) and lipoic acid and the $\lambda_{max}$ was observed around 540-580nm for GSH capped and 560-620nm for lipoic acid (LA) capped gold nanoparticles. The change in the color of the colloid seen before and after capping from wine red to blue for GSH and dark blue for lipoic acid capped nanoparticles [7]. The application of gold nanoparticles are based on combining two principles:

a. Surface functionalization for providing the colloidal stability and biocompatibility of nanoparticles, the molecular recognition of conjugates, efficient endocytosis, etc.

b. The corresponding excitation of plasmon resonances in the visible or near-IR region in order to obtain unique optical properties (Figure 2) [1,8].

The most popular ligand for surface functionalization is thiolated poly(ethylene glycol)(PEG-SH), which forms a covalent bond (chemisorption) with the surface atoms of gold nanoparticles. Chemisorption is a kind of adsorption which involves a chemical reaction between the surface and the adsorbate. New chemical bonds are generated at the adsorbant surface. The strong interaction between the adsorbate and the substrate surface creates new types of electronic bonds. PEG molecules were also used as linkers for further labeling with a probe molecules for certain targets. Other substances such as albumin, maltodextrin, sodium alginate, immunoglobulin, maltose, conventional surfactants, oligosaccharides, DNA oligonucleotides, oligopeptides, gum arabic and so on can be also used for the stabilization of spherical nanoparticles. Gold anisotropic nanoparticles (nanorods) are initially produced with some surfactants such as CTAB molecules which are physically adsorbed on the particle surface. To make them biocompatible the surfactants molecules (ligands) are easily replaced with PEG-SH reagents [9]. The ligand exchage is also used in the case of less stable gold nanoparticles. Otherwise they will aggregate at the moment of injection under conditions of elevated ion concentration and the presence of biomolecules, inevitably leading to differences in the gold nanoparticle circulation kinetics in the blood stream. Moreover, the use of biocompatible ligands with probe molecules can increase gold nanoparticle accumulation in a target organ as they are discussed below.

## Biodistribution Kinetics

### Particle (stabilizer) surface effect

It was reported that the unmodified (bare) 20-nm AuNPs concentratein 28 organs, the feces and urine of rats for 2 months after a single intravenous AuNP administration at a very low dose [10]. These nanoparticles predominantly accumulated in the liver (80%) and spleen (12%). Smaller amounts of gold were found in the kidneys (5%) and testicles (below 1%). The interaction of unstable nanoparticles with biomolecules probably leads to the particle agglomeration and their concentration in the liver. Similar nonfunctionalized 18-nm AuNPs and the particles coated also with polyacrylamide displayed no cytotoxicity to human breast adenocarcinoma cells [11]. No cytotoxic effect was also reported for smaller 10-nm unmodified AuNPs towards dendritic cells by Villiers et al. [12].

Bergen et al. [13] have used bare and nanoparticles covered bynonionic stabilizers based on PEG with diameters of 50, 80, 100, and 150 nm to study the biodistribution kinetics. Nonionic stabilizers provides particles without the charge. They used also various additives and mixed stabilizing systems such as PEG alone, PEG+ galactoseor albumin. The additives, however, might providepartial positive or negative charges. The level of AuNPs in the mouse blood after injection was maximal for particles coated with PEG. Furthermore, the level of gold for the PEG-coated particles with sizes of 50,80 and 100 nm was considerably larger than that for the 150-nm particles. Albumin protected AuNPs are approximately by two orders of magnitude lower than for the AuNPs protected with PEG molecules. However, the level of gold in the blood for the AuNPs conjugated with galactose-PEG conjugate was minimal, being by three and more orders of magnitude lower than PEG without galactose:

AuNP-PEG>> AuNP-PEG-albumin >> AuNP-PEG-galactose

These results indicate that the terminal groups of the organic shell govern their interaction activities. The behavior with the terminal galactose units was explained by the fact that the galactose molecules served as a target for liver hepatocytes. However, this conclusion is completely attributable only to conjugates of 50-nm particles, because the ratio of the gold concentration in hepatocytes to the gold concentration in nonparenchymatous cells for them was about 2.5. Moreover, only for these particles was the level of gold in hepatocytes 16-fold higher for the conjugate AuNPs-50 + galactose–PEG-

SH than in the control, AuNPs-50 + PEG-SH. Thus, these results unambiguously demonstrate *in vivo* the specific delivery of a complex of 50-nm particles with surfaces modified by galactose–PEG-SH to hepatocytes. MTT testing did not detect any cytotoxicity of 15-nm PEG-coated nanoparticles (up to a concentration of 100 μg/ml) or 30-nm gold particles to the HepG2 cell line, either [14]. The distribution kinetics of much smaller albumin coated 16-nm gold nanoparticles in pigs were followed by Darien et al. [15]. Herein the largest amount of particles (ca. 75%) were accumulated in the lungs followed by the liver (24%) and blood plasma (below 1%). The absence of cytotoxicity was observed also with 18-nm AuNPs coated with folic acid in HeLa cells [16,17]. The clearance halftimes of the PEG-decorated 20-, 40-, and 80-nm AuNPs from mouse blood were estimated by Zhang et al. [18]. They showed that the halftimes increased with decreasing the particle size:

1 min (for 80 nm AuNP) < 10 (40 nm) < 30-40 (20 nm).

These results indicate that the particle elution time or the length of pathway is inversely proportional to the particle size. The smaller the nanoparticles, the stronger the interaction of nanoparticles with the surrounding molecules. Thus, the tray of small nanoparticles is much longer than the tray of large nanoparticles or the small nanoparticles interact with the higher number of biomolecules, salts and ions. Moreover, the 80-nm AuNPs entered the liver and spleen as early as after 10 min, being undetectable in the blood, kidneys, bladder, and intestine, whereas the 20-nm particles circulated in the blood longer; accumulated in the liver and spleen to a lesser degree; and were detectable in the heart, kidneys, and intestine. In addition, only 20-nm particles accumulated in the tumor tissue, which is naturally explainable by longer circulation and the effect of retention in the tumor with an elevated blood supply and the increased colloidal stability.

Biodistribution kinetics of the PEG-coated gold nanorods (AuNRs, aspect ratio 6) investigated by Niidome et al. [19] indicated that ca. 50% of the PEG-coated AuNRs intravenously administered to mice were detectable in their blood after 30 min, whereas most of the AuNRs stabilized with CTAB molecules were detectable in the liver. Traces of PEG- coated AuNRs were identified in their lungs, spleen, and kidneys. After 1 day, the PEG-coated AuNRs were detectable only in the liver. Thus, the interchange of CTAB molecules with PEG ones drastically changed the biodistribution pattern mainly at the earliest stages. The PEG-coated particles circulated by one order of magnitude longer and, correspondingly, considerably more slowly accumulated in the liver. This difference can be discussed in terms of the different colloidal stability. The stability of AuNRs covered by adsorbed CTAB molecules is much lower than those stabilized by chemisorbed PEG molecules. In the former case the increased agglomeration of nanoparticles in the blood leads to the AuNRs accumulation in the liver. This is not the case with the PEG-coated AuNRs.

The further parameter that can influence the biodistribution (the particle retention in and distribution between the organs) is the coating shell density as it was discussed in the next work by Niidome et al. [19]. Herein an increase in the degree of coating decreased the gold concentration (a percentage of the dose) in the spleen and increased in the liver and tumor. At a high PEG/gold molar ratio (over 1.5), the amount of gold per unit weight was higher in the tumor than in the liver. Similarly, an increase in the dose to approximately 40 μg/mouse yielded a high level of gold nanorods in the tumor. The role of the PEG coating on the biodistribution can be discussed as follows: Theoretically one can imagine two or three limiting cases of AuNR-PEG conjugate configuration: PEG can be wrapped around the nanoparticle bound in random coiled shape, or bound in stretched shape pointing perpendicular to the surface (Figure 3). This configuration is a function of PEG length and number, the presence of additives (e.g. salt,...), temperature and biological conditions. The conformation and packing of the PEG can strongly influence the accessibility of the polymer chains for interaction (the complex formation, hybridization,...) and the particle mobility.The mobility of the PEG-coated gold nanoparticles is always retarded by the increased ligand density which is directly related to the particle retention and distribution between organs. Furthermore, the nanoparticles with PEG wrapped around strongly interact between-themselves to larger aggregates and concentrate in the liver.

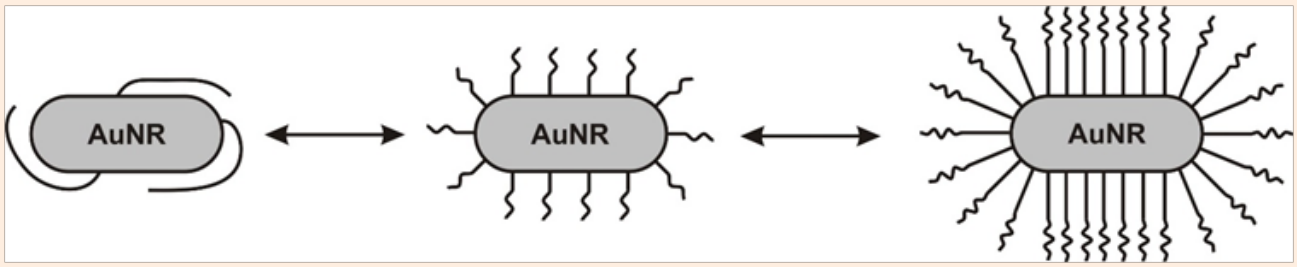


Figure 3: Different possible configurations of PEG molecules attached to the surface of gold nanoparticles.

The next study also points out on the particle surface density as an important parameter for the biodistribution kinetics. Herein, an increase in the peptide molecules (ligand density) from 30 to 150 molecules per 5-nm gold nanoparticle decreased the cell survival rate from 98 to 66% [20]. The 13-, 30- and 60-nm AuNPs covered with CALNN peptides showed a similar behavior [21]. The survivability of HeLa cells (according to trypan blue test) at AuNP concentrations of 0.02–0.08 nM was 80–95% and decreased to 60% at a AuNP concentration of 0.16 nM and to less than 10% at 0.32 nM. The increase in the particle surface density (CALNN molecules) favours the interaction and penetrationof nanoparticles into cells.

The biodistribution kinetics of ca. 120-nm core@shell -silica (ca 110 nm)@gold (gold nanoshell (ca. 10 nm) (AuNS))-hybrid nanoparticles were followed in mice by James et al.

[22]. PEG-coated AuNSs were intravenously administered to healthy mice and mice with transplanted tumors. Hybrid AuNSs mainly accumulated in the spleen characterized with a very slow clearance. A similar behavior was observed for the liver, but at an approximately by one order of lower accumulation amount level. A slow AuNSs clearance from the organs of the reticuloendothelial (RE) system was also observed with PEG-covered nanorods [23]. These results indicate that the common PEG shell governs the biodistribution of gold nanoparticles independent of their shape. The inert silica nanoparticles are speculated to be resposible for high level of nanoparticles within some organs and a very slow clearance rate. A high AuNS level in the blood was observed for less than 1 day, and most of the particles were eliminated from the lungs by the end of day 1 and then slowly decreased. In the case of mice with transplanted tumors, the maximal accumulation contrast was observed 1 day after injection. It is important to note that the unfunctionalized AuNSs accumulate in the tumor exceeded manytimes the corresponding levels in the blood, lung, muscles, kidneys, brain, and bones, except, of course for the spleen and liver.

PEG-coated AuNSs with diameters of 15, 50 nm and 160 nm core@shell silica@gold (gold nanoshell, silica core particle diameter of 120 nm) (1 day) after intravenous administration into rats accumulated in brain, kidneys and lungs [24]. On the contrary a high (size 50 and 160 nm) accumulation of 50 and 160 nm nanopartices was observed in the liver (ca. 60%) and somewhat lower in spleen (ca. 30%). Unlike the data of James et al. [22], the gold levels in the spleen were comparable for 50-nm AuNPs and 160-nm AuNSs. This difference can be discussed in terms of different animal models (mice in and rats in), significantly different doses 10 μg/g [22] and 1.3 μg/g [24], different particle shapes, surface particle composition and the particle nature. For example the interaction of particles with biomolecules will differ for silica and gold atoms. However, we must take into consideration also the particle size distribution which may differ for both cases.

The biodistribution kinetics for AuNPs functionalized by polyvinylpyrrolidone (PVP) and bovine serum albumin (BSA) molecules (without charge)was followed by Hardonk at al. [25] with different nanoparticle sizes in *in vivo* experiments on the cancer cells. The full-length BSA precursor protein is 607 amino acids (AAs) in length. An N-terminal 18-residue signal peptide is cut off from the precursor protein upon secretion, hence the initial protein product contains 589 amino acid residues. An additional 4 amino acids are cleaved to yield the mature BSA protein that contains 583 amino acids (MW = 66.5 kDa, pH ~5.5). Both sets of neutral nanoparticlesshowed the similar biodistribution kinetics and no cytotoxicitybecause both have no charge (BSA might be slightly positively charged). Furthermore the 7-nm gold nanoparticles decorated with polyvinylpyrrolidone also had no cytotoxic effect on the human embryonic kidney or human breast cancer cells [26]. Similarly 20-nm BSA-decorated AuNPs towards HeLa cultures were without any cytotoxic effect [27]. A similar behavior was detected by LDH testing with 15-nm BSA-decorated AuNPs coated with BSA to 3T3/NIH cells by a MTT test [28].

In the next investigation the 15-80 nm AuNPs coated with gum arabic and maltose modifiers (stabilizers) were used. Gum arabic is a complex mixture of glycoproteins and polysaccharides. It was historically the source of the sugars arabinose and ribose, both of which were first discovered and isolated from it, and are named after it. Maltose is a disaccharide formed from two units of glucose joined with an α(1→4) bond, formed from a condensation reaction. The former nanoparticles predominantly accumulated in the liver, whereas the later particles accumulated in the lungs. The much larger moleculare weight of the former indicates that the gum arabic provides much larger nanoparticles. This may be the result why the former accumulate in the liver and the latter (smaller) in the lungs. The small 17-nm gold nanoparticles were observed in hepatocytes, whereas large 79-nm ones did not follow the same pathway. Further analyses showed that AuNPs were also detectable in feces after administration and identified also in the Kupffer cells. Similarly the small 15–20 nm gold nanoparticles coated with gum arabic and maltose, however, displayed different accumulation patterns in the blood, tissues (liver and lungs), and urine; moreover, the difference reached 50% and higher [29]. Less stable nanoparticles accumulate in liver and urine and more stable in lungs. This differenceis supposed todepend on the surface ligand density which is higher for the maltose covered nanoparticles.

The uptake of 14, 50, and 74 nm sized gold nanoparticles covered by citric acid entities into HeLa cells led to the unexpexted results [30]. Ligands based on citric acid derivatives belong to weak capping agents and they can be exchangedeasily by various biomolecules within the cells. All nanoparticles were reported to be absorbed by the cells but 50-nm spheres were more quickly taken up by endocytosis than both the smaller and larger sizes. This behavior could be discussed in terms of different surface ligant densities (accesibility of functional groups for interaction) and shapes of nanoparticles. Herein cells absorb 50-nm nanoparticles keeping a certain configuration of citric acid on the particle surface. This is not true for the other two nanoparticles. Furthermore, citric acid ligands are weak capping agents or surfactants and therefore the size and shape can be varied within the cells according to the pH value and the type of functional group within the cells. The citric acid stabilized gold nanoparticles was further modified with transferrin to estimate the rate of exocytosis of transferrin-coated gold nanoparticles. The rate of exocytosis was determined to be size-dependent with increased accumulation of large gold nanoparticles within the cell [31].

In the next study the 18-nm AuNPs covered with three different surfactants (modifiers)citrate, biotin and CTAB were used to asses the cytotoxicity to K562 cell [32]. Citrate and biotin covered nanoparticles were without cytotoxicity to a concentration of 250 μM versus particles functionalized with CTAB, which were toxic at a concentration as low as 0.05 μM but lost their toxic properties after being washed from CTAB. The toxicity of the conjugate was attributed to the presence of free CTAB in the continuous phase. The chemisorbed citrate ions (three corboxylic groups) and biotin (biotin is a heterocyclic, S-containing monocarboxylic acid) are located on the particle surface. Sodium citrate covered gold particles, on the contrary, werereported to get cytotoxicity. This migh be attributed to the free citrate ions within the media [33]. Similar to a surfactant type, surface properties might play a key role in the cytotoxicity of the same particles. In particular, the cytotoxicity of positively and

negatively charged 2-nm AuNPs to COS-1 cells and erythrocytes was investigated by Fuente et al. [34]. The positively charged nanoparticles were sevenfold more toxic when compared with negatively charged particles.

Wang et al. [23] prepared positively charged AuNRs (CTAB-coated AuNRs with AR=4.3, 56 × 13 nm) and followed their biodistribution among different organs in the rats. The particle surface charge was varied by the addition of protein selecting BSA. The interaction od AuNRs with BSA led to the neutralization of the particle charge and the formation of charge neutral conjugates. Therein, the sign of the AuNR zeta-potential changed while preserving their stability. The positive charged particle surface ($CTA^+$ ions) was neutralized by negatively charged BSA molecules. The data on the kinetics of particle accumulation (from 0.5h to 28 days) demonstrated a rapid decrease in AuNR concentration in the blood at the very initial moment with a subsequent gradual decrease over several days, as well as a significant accumulation in the liver (to 60% of the dose) and spleen (to 1.3%).

The AuNR amount remained almost unchanged for nearly one month. A strong initial accumulation in the lungs (about 2.5%) was accompanied by a gradual decrease in the level to 0.6% of the dose by day 28. Furthermore AuNRs were reliably detectable in the brain. Thus, if even one of the sizes is small (a AuNR thickness of 13 nm), that is sufficient for it to pass through the BBB with its critical size of 20nm. We speculate that the interaction of BSA-covered AuNRs with blood ingradients initiate their agglomeration and accumulation in the liver. The gradual decomposition of the AuNR-CTAB-BSA (the release of BSA) or exchange of the present ligands leads to the formation of charged and more stable nanoparticles. Furthermore the nanoparticles with the broad particle size distribution might lead to the accumulation of the large particles in the liver and the small ones – more stable – in the blood and in the brain as well.

It has been shown that the gold nanorods coated with PEG display a lower cytotoxicity, penetrate into cells to a lesser degree, and are more stable in culture medium when compared with the AuNRs modified with poly(sodium styrene sulfonate) (PSS) [35]. In addition to PEG and PSS, other substances are also used to decrease nanorod cytotoxicity via CTAB substitution or the creation of an additional surface layer, namely, phosphatidylcholine [36].

Alkilany et al. [37] assessed the cytotoxicity of gold nanorods covered by CTABs in the human colonic carcinoma cell (HT-29) culture. Other coating of the nanorods with polymers such as polyacrylic acid (PAA) or polyallylamine hydrochloride (PAH) significantly decreased their cytotoxicity. Thus, the replacing CTAB with nontoxic stabilizers, such as PEG, PSS, PAA, PAH, or others, is one efficient method for decreasing the cytotoxicity of CTAB-stabilized AuNRs. In the next work the CTAB-coated rods displayed a high cytotoxicity to HeLa cells at a very small dose (80% killed cells) [9]. However, 95% of the viable cells were observed at a nanorod concentration of 0.5 mM after thiolated poly(ethylene glycol) (PEG-SH) was substituted for CTAB. This behavior is discussed in terms of a decrease in the cell-penetrating ability of PEG-coated nanorods [38]. However several authors [39,40] observed a considerable decrease in the cytotoxicity of nanorods not only after CTAB substitution with PSS, but also after triple washing, whereas rods without washing were rather toxic. Comparing this with addition of only free CTAB (without any particles) demonstrates that the action of triply washed AuNRs is approximately similar to that of 10 μm of free CTAB, while PSS-coated particles are analogous in toxicity to 1 μm of CTAB or to the control. The main difficulty in assessing the cytotoxicity of CTAB-coated AuNRs is their low stability and trend for aggregation, which is most certainly accompanied by additional CTAB release. A decrease in the cytotoxicity of CTAB-coated AuNRs after being washed with distilled water from CTAB molecules contained in a solution and after conjugation with immunoglobulins is also reported [41]. The authors infer that the toxicity of such systems is determined by free CTAB, whereas the CTAB-coated AuNRs are not cytotoxic.

The distribution kinetics of hollow (without a silica core) gold 30-nm nanoshells (AuNS) coated with immunoglobulins was studied in mice with transplanted tumors [42]. Therein the maximal AuNS accumulation was detectable in the liver, spleen, and kidneys, amounting to approximately 20% of the dose in each; considerably smaller gold quantities were observed in the heart, lungs, stomach, small intestine, muscles, and bones (ca. 5% per each organ); about 10% of the AuNSs accumulated in the tumor. The immunoglobulin covered nanoshells prefer kidneys and are characterized by a lower clearance for other organs (smaller amounts of gold were also obtained in other organs).

## Particle size effect

Subnanoparticles and nanoparticles of particle diameters 0.8 nm (eight gold atoms aggregate), 1.2 nm (35 atoms), 1.4 nm (55 atoms), and 1.8 nm (150 atoms), as well as 15-nm nanoparticles stabilized with triphenylphosphine derivatives were used to studythe size effect on the cytotoxicity in four cell lines (HeLa, Sk-Mel-28, L929, and J774A1) [43]. The most cytotoxic, according to an MTT test, were 1.4-nm clusters displaying the inhibitory concentration $IC_{50}$ ca. 40 μM. The $IC_{50}$ values for somewhat smaller 0.8 and 1.2-nm and somewhat larger 1.8-nm clusters were considerably higher, namely, 250, 140 and 230 μM, respectively. The 15-nm AuNPs did not display any cytotoxicity, even at very high concentrations. In addition, the 1.4-nm clusters induced cell necrosis and those 1.2-nm clusters induced apoptosis. The similar toxicity of 1.4-nm gold clusters to healthy and tumor human cells were also assessed by Tsoli et al. [44]. The high toxicity of 1.4-nm $Au_{55}$ clusters might be attributed to a size similarity to B-form DNA [2]. Thus, these works suggest that a transition to the sizes of classical colloid particles (15 nm) drastically decreases cytotoxicity when compared with atomic clusters of about 1-2 nm, which are capable of irreversibly binding to DNA, protein and, possibly, other key molecules. We must take into account the fact that the properties of large gold particles are similar to the bulk gold. On the contrary small AuNPs, ca. 1-2 nm, exhibit nontraditional properties including the high reactivity. Furthermore the intercalation of small nanoparticles into the dsDNA can be one of possible effects. We should include also the different water-slubility of nanoparticles and the degradation of nanoparticles with various sizes due to the Oswald wripening. The smaller the nanoparticles the larger the decompostion of gold nanoparticles. Furthermore the presence of free triphenylphosphine molecules in the solution and/or the low surfactant density on the particle surface could

be a further important key parameter.

Nanoparticles of 1.4 nm diameter exhibited increased cytotoxicity ($IC_{50}$=30-46μM), whereas subnanoparticles of 0.8 nm and nanoparticles 1.2 and 1.8 nm were four to six-fold less toxic. Here in we can speculate thatafter administration 0.8 nm gold nanoparticles agglomerate and their elimination increased and become less cytotoxic. Furthermore, the presence of nospherical nanoparticles might influence the penetration ability of the sample as well as its cytotoxicity. Large sizes (15 nm), as expected, with low penetration into cells exhibited no cytotoxicity even at high concentrations (6.3 mM) [45]. A similar behavior wasobserved with other very small 1-2 nm AuNPs that were highly toxic in all healthy or cancer cells. In contrast, somewhat larger 4, 12 and 18 nm gold nanoparticles did not exhibit any inherent toxicity to human K562 leukemia cells. The high penetration ability of small nanoparticles into cells, the considerable penetration and accumulation of AuNPs, for example, in the different animal or human organs (liver, spleen, lungs,..) and their slow elimination areall connected with their high toxicity. The 4-nmgold nanoparticles were reported toenter via the digestive tract and distribute among several organs [45]. The penetration into various tissues via the digestive tract considerably decreased with an increase in the particle size (10,28 and 58nm). The 4-nm particles were maximal (about 75%) in the kidneys and about 25% in other organs (small intestine, lungs, stomach, spleen, and liver) and also show the high penetration efficiency into the brain (thus, AuNPs can pass through the BBB) [46].

The fate of 10-50nm gold nanoparticleswere followed after i.v. injection of colloidal sample in mice. As expected small particles were found to disperse quickly to almost all tissues, mainly accumulating in the liver, lungs, spleen, and kidneys. Accumulation of large particles (100-200 nm) was depressed into many organs and they accumulated mainly in the liver, lungs, spleen, and kidneys, but they were not as widely dispersed into other tissues as were the small particles. These studies supported above-mentioned results of gold colloid effects ona size-dependent distribution concerning of increased toxicity of small gold nanoparticles [3,47]. Hardonk et al. [25] and Sadauskas et al. [48] reported on the accumulation of gold nanoparticles of different sizes in different mice organs and foundthat Kupffer cells playimportant role in gold nanoparticles clearance from the body in mice after i.v. injection of 2- and 40-nm gold nanoparticles. After injection gold nanoparticles accumulated mainly in liver macrophages (90%), whereas their amount in the spleen macrophages was considerably smaller (10%). Presumably, TEM was not enough sensible for detecting gold nanoparticles accumulated in the other organs (kidneys, brain, lungs, adrenal glands, ovaries, and placenta). Furthermore, studied nanoparticles penetrated only into the phagocytic cells (first and foremost, Kupffer cells), failed to cross the placental and bloodbrain barriers (BBBs), and small 2-nm particles could be excreted with urine.

Note that the gold concentration in the brain exceeded the gold concentration in the experiment with 4-nm particles by one order of magnitude and was 20-fold for that with 10-nm particles. Thus, both studies unambiguously confirmed that particles with a diameter of 10 nm or smaller could pass through the BBB. The detection of AuNPs smaller in diameter in the brain suggests that the AuNP penetration through the BBB is critically size-dependent, with the upper boundary for penetration being about 20nm [46]. It was assumed that this transfer involveinteractions with different proteins such as apolipoprotein A-I, which attached to the nanoparticle surface via the SR-BI receptor localized to the BBB. The apolipoprotein adsorption on AuNPs can enhance the penetration of AuNPs with the sizes smaller than 20 nm through the BBB. Particles 100 nm in size were undetectable in retinal tissues, whereas 20-nm particles were found in almost all the retinal layers, including neurons (70%), endothelium (17%), and glial cells (8%) [46]. Further study [49] discovered that 40-nm gold nanoparticles were localized to lysosomes (endosomes) and could stay there for up to 6 months. The 13-nm gold particles accumulated in the liver and spleen after i.v. injection by much larger amount than in the experiment with administration via the digestive tract [36,50].

10, 50, 100, and 250 nm gold nanoparticles accumulated to the greatest degree in the liver and spleen [3]. Small 10-nm particles were identified in the kidneys, testicles, thymus, heart, lungs, and brain. Similar behavior was observed by Sonavane et al. [51] who demonstrated a considerable accumulation of particles of all sizes (15, 50, 100, and 200 nm) in the liver. However, Sonavane et al. [51] also reported that 15-nm particles displayed a considerable accumulation in the kidneys and lungs and only the largest 200 nm AuNPs were prevalent in the spleen along with the liver.

The cytotoxic and immunogenic actions of 3.5 nm gold particles were assessed to the macrophage cell culture RAW 264.7 [52]. Similar results were obtained for 3 nm AuNPs, 5nm, 5, 12, 20, 30, 50, and 70nm, 3, 5, 8, 12, 17, 37, 50, and 1200nm, 4 and 13nm, and 40nm 112 [53-58]. Taking into account the above-mentioned data, it could be possible to expand the boundaries to both the lower level (to 3 nm) and larger particles up to 100 nm to avoid a toxic AuNP effect, if we are considering a limited dose of about $10^{12}$ particles/ml. However, the citrate covered 5-20 nm AuNPs were not toxic independent of particle concentration.

## Other parameters

Various animal cell cultures are used for an *in vitro* assessment of cytotoxicity, such as human skin fibroblasts (HeLa), human leukemia cells (K562), human hepatocarcinoma cells (HepG2), human breast adenocarcinoma cells (SK-BR-3), and some others. The cytotoxicity, however, can also depend on the cell type [59]. For example, 33-nm AuNPs are not cytotoxic to hamster kidney (BHK-21) or human hepatocellular carcinoma (HepG2) cell lines (according to MTT tests) but were toxic to the human lung carcinoma (A549) cell line. Herein the toxicity was directly proportional to the dose of administered nanoparticles. A neurotoxic effect of AuNPs on neuroblastoma cells was also demonstrated [60].

The toxic effects of 5, 15, and 30 nm AuNPs on human bone marrow stem cells (hBMSC line) and human hepatocarcinoma (HuH-7) were reported by Fan et al. [61]. The cytotoxicity was assessed by MTT testing for 5 days using various concentrations of nanoparticles. Both cultures displayed over 80% of live cells after the addition of 15- and 30-nm particles at concentrations

of up to 70 mg/ml. However, the 5-nm particles added at a concentration of only 30 μg/ml reduced the rate of viable cells to below 60%. Thus, according to toxicity in this model, the lower size limit was about 15 nm. Concentrations of 30 μg/ml for 5-nm particles (150μM Au or $2.5\times10^{13}$ particles/ml) seem to be too high to speak about a genuinely toxic effect of small doses. Therefore, it is believed that the results of Fan et al. [61] fit to Klebsov' conclusion well when assuming a value of about $10^{12}$ particles/ml to be the upper limit of particle number concentration. Singh et al. [62] have considered the work on cyto- and genotoxicities of the AuNPs coated with a glycolipid. It was demonstrated that 10-nm AuNPs (a concentration of $2\times10^{12}$ particles/ml) at concentrations up to 100μM had no cytotoxic (MTT test; 80% cell survival rate for 3h) or genotoxic (assessment of DNA damage by comet analysis) effects.

Several analytical methods have been used to follow the fate of gold nanoparticles in different animal and human cells and organs. Among them mainly TEM, surface plasmon resonance (SPR) spectroscopy, neutron activation analysis (INAA or NAA), mass spectrometry with inductively coupled plasma (ICP-MS), atomic adsorption spectrometry (AAS) were used. For example, ICP-MS yields a detection limit of about 0.001μg/kg [23], which is quite sufficient for an accurate estimate of particle accumulation and location in bodies. An available toolkit for detecting gold in various organs (RA, INAA, ICP-MS, and AAS), AuNP localization and identification at cellular (TEM and EDX (Energy Dispersive X-ray Spectrometry)) and structural (XAS (X-ray absorption spectroscopy)) levels, and assessing *in vitro* cytotoxicity (MTT and WST-1) has been tested and used for the required characterization.

## Conclusion

The interaction of unstable (bare) nanoparticles with biomolecules increased the particle agglomeration and their concentration in the liver, that is, the half times of nanoparticles decreased. The level of gold for the PEG-coated nanoparticles in the blood was considerably larger than that for the ionic (CTAB or anionic) stabilizer coated nanoparticles. A similar behavior was observed for the PEG-coated nanoparticles conjugated with additives such as albumin, galactose, arabic gum,... The concentration of nanoparticles in the blood is inversely proportional to the molecular weight of the additive. The shell density of gold nanoparticles relates to both the colloidal stability and the cytotoxicity. Functional (ionic) surfactants (modifiers) have a pronounced effect on the distribution pattern not only by changing the circulation time in the blood stream but also changing the nature of gold conjugates. A correctly selected (functional) stabilizer can yield a considerable difference in accumulation in the target organ. Examples include an increased accumulation of galactose-containing PEG or maltose coated AuNPs in the liver hepatocytes and an increased accumulation of nanoparticles conjugated with TNF in a transplanted solid tumor. The positively charged nanoparticles were sevenfold more toxic when compared with negatively charged particles, and the latter were more toxic than the neutral nanoparticles. The clearance half times of the PEG-decorated AuNPs from blood increased with decreasing the particle size. These results indicate that the particle elution time or the length of pathway is inversely proportional to the particle size. The smaller the nanoparticles, the stronger the interaction of nanoparticles with the surrounding molecules.

Thus, the tray of small nanoparticles is much longer than the tray of large nanoparticles or the small nanoparticles interact with the higher number of biomolecules, salts and ions. Thus, the size of gold nanoparticles is a further factor that determines their biological fate. First, the organs of the reticuloendothelial system are the main target for the accumulation of AuNPs; moreover, the uniformity of biodistribution increases with a decrease in particle size. The lower the nanoparticles the higher the uniformity of biodistribution. Third, AuNPs with diameters of 1–2 nm have a potentially high toxicity due to their possible irreversible binding to key biopolymers. Sub nanoparticles and small gold particles penetrate deeply into tissues, exhibit high elution and retention pathway and are cytotoxic. The functional tissues present high activity to particle surface which favor their possible irreversible binding to biopolymers. The toxicity of the AuNPs is determined by their ability to irreversibly bind to key biomolecules (DNA and others) and change the functioning of cellular molecular processes.

Overall experimental data suggest an inference complying with the majority of works, namely, that if the upper limit of the particle concentration does not exceed critical value, then colloidal AuNPs do not display cytotoxicity down to small sizes of 3–5 nm. One should study the correlations between the parameters of particles (size, shape, and functionalization), experimental parameters (model; doses; administration route and time pattern; duration of observations; and examined organs, cells, sub-cellular structures, etc.), and the observed biological effects. Further, special attention should be paid to the interaction between AuNPs and additives, and AuNP conjugates with the cells of the immune system, because this interaction can cause a nonspecific immune response and change not only the biodistribution of nanoparticles, but also the subsequent response of the organism.

## Acknowledgement

This research was supported by APVV-0125-11 and VEGA 2/0040/14 and 2/0152/13 projects.

## References

1. Khlebtsov NG, Dykman LA (2010) Optical properties and biomedical applications of plasmonic nanoparticles. Journal of Quantitative Spectroscopy and Radiative Transfer 111(1): 1-35.
2. Semmler-Behnke M, Kreyling WG, Lipka J, Fertsch S, Wenk A, et al. (2008) Biodistribution of 1.4- and 18-nm gold particles in rats. Small 4(12): 2108-2111.
3. De Jong WH, Hagens WI, Krystek P, Burger MC, Sips AJ, et al. (2008) Particle size-dependent organ distribution of gold nanoparticles after intravenous administration. Biomaterials 29(12): 1912-1919.
4. Jana NR, Gearheart L, Murphy CJ (2001) Seed-mediated growth approach for shape-controlled synthesis of spheroidal and rod-like gold nanoparticles using a surfactant template. Adv Mater 13(18): 1389-1393.
5. Capek I (2004) Preparation of metal nanoparticles in water-in-oil (w/o) micro emulsions. Adv Colloid Interface Sci 110(1-2): 49-74.

6. Zhang HL, Qiao FY, Liu J, Li FR, Kong XL, et al. (2008) Antibody and DNA dual-labeled gold nanoparticles: Stability and reactivity. Applied Surface Science 254(10): 2941-2946.

7. Ahirwal GK, Mitra CK (2009) Direct electrochemistry of horseradish peroxidase-gold nanoparticles conjugate. Sensors (Basel) 9(2): 881-894.

8. Capek I (2013) Preparation and functionalization of gold nanoparticles. J Surface Sci Technol 29(3-4): 1-18.

9. Niidome T, Yamagata M, Okamoto Y, Akiyama Y, Takahashi H, et al. (2006) PEG-modified gold nanorods with a stealth character for in vivo applications. J Control Release 114(3): 343-347.

10. Balasubramanian SK, Jittiwat J, Manikandan J, Ong CN, Yu LE, et al. (2010) Biodistribution of gold nanoparticles and gene expression changes in the liver and spleen after intravenous administration in rats. Biomaterials 31(8): 2034-2042.

11. Salmaso S, Caliceti P, Amendola V, Meneghetti M, Magnusson JP, et al. (2009) Cell up-take control of gold nanoparticles functionalized with a thermo responsive polymer. J Mater Chem 19(11): 1608-1615.

12. Villiers CL, Freitas H, Couderc R, Villiers MB, Marche PN (2010) Analysis of the toxicity of gold nanoparticles on the immune system: effect on dendritic cell functions. J Nanopart Res 12(1): 55-60.

13. Bergen JM, von Recum HA, Goodman TT, Massey AP, Pun SH (2006) Gold nanoparticles as a versatile platform for optimizing physicochemical parameters for targeted drug delivery. Macromol Biosci 6(7): 506-516.

14. Kim D, Park S, Lee JH, Jeong YY, Jon S (2007) Antibiofouling polymer-coated gold nanoparticles as a contrast agent for in vivo X-ray computed tomography imaging. J Am Chem Soc 129(24): 7661-7665.

15. Darien BJ, Sims PA, Kruse-Elliott KT, Homan TS, Cashwell RJ, et al. (1995) Use of colloidal gold and neutron activation in correlative microscopic labeling and label quantitation. Scanning Microsc 9(3): 773-780.

16. Khan JA, Pillai B, Das TK, Singh Y, Maiti S (2007) Molecular Effects of Uptake of Gold Nanoparticles in HeLa Cells. Chem Biochem 8(11): 1237-1240.

17. Li G, Li D, Zhang L, Zhai J, Wang E (2009) One-Step Synthesis of Folic Acid Protected Gold Nanoparticles and Their Receptor-Mediated Intracellular Uptake. Chemistry 15(38): 9868-9873.

18. Zhang G, Yang Z, Lu W, Zhang R, Huang Q, et al. (2009) Influence of anchoring ligands and particle size on the colloidal stability and in vivo biodistribution of polyethylene glycol-coated gold nanoparticles in tumor-xenografted mice. Biomaterials 30(10): 1928-1936.

19. Niidome T, Akiyama Y, Shimoda K, Kawano T, Mori T, et al. (2008) In vivo monitoring of intravenously injected gold nanorods using near-infrared light. Small 4(7): 1001-1007.

20. Ryan JA, Overton KW, Speight ME, Oldenburg CN, Loo LN, et al. (2007) Cellular uptake of gold nanoparticles passivated with BSA-SV40 large T antigen conjugates. Anal Chem 79(23): 9150-9159.

21. Sun L, Liu D, Wang Z (2008) Functional gold nanoparticle-peptide complexes as cell-targeting agents. Langmuir 24(18): 10293-10297.

22. James WD, Hirsch LR, West JL, O'Neal PD, Payne JD (2007) Application of INAA to the Build-up and Clearance of Gold Nanoshells in Clinical Studies in Mice. J Radio anal Nucl Chem 271(2): 455-459.

23. Wang L, Li YF, Zhou L, Liu Y, Meng L, et al. (2010) Characterization of gold nanorods in vivo by integrated analytical techniques: their uptake, retention, and chemical forms. Anal bio anal chem 396(3): 1105-1114.

24. Terentyuk GS, Maslyakova GN, Suleymanova LV, Khlebtsov BN, Kogan BY, et al. (2009) Circulation and distribution of gold nanoparticles and induced alterations of tissue morphology at intravenous particle delivery. J Biophotonics 2(5): 292-302.

25. Hardonk MJ, Harms G, Koudstaal J (1985) Zonal heterogeneity of rat hepatocytes in the in vivo uptake of 17 nm colloidal gold granules. Histochemistry 83(5): 473-477.

26. Zhou M, Wang B, Rozynek Z, Xie Z, Fossum JO, et al. (2009) Minute synthesis of extremely stable gold nanoparticles. Nanotechnology 20(50): 505606.

27. Tkachenko AG, Xie H, Liu Y, Coleman D, Ryan J, et al. (2004) Cellular trajectories of peptide-modified gold particle complexes: comparison of nuclear localization signals and peptide transduction domains. Bioconjugate Chem 15(3): 482-490.

28. Murawala P, Phadnis SM, Bhonde RR, Prasad BLV (2009) In situ synthesis of water dispersible bovine serum albumin capped gold and silver nanoparticles and their cytocompatibility studies. Colloids Surf B Biointerfaces 73(2): 224-228.

29. Fent GM, Casteel SW, Kim DY, Kannan R, Katti K, et al. (2009) Biodistribution of maltose and gum arabic hybrid gold nanoparticles after intravenous injection in juvenile swine. Nanomedicine 5(2): 128-135.

30. Chithrani BD, Ghazani AA, Chan WCW (2006) Determining the size and shape dependence of gold nanoparticle uptake into mammalian cells. Nano Lett 6(4): 662-668.

31. Chithrani BD, Chan WCW (2007) Elucidating the mechanism of cellular uptake and removal of protein-coated gold nanoparticles of different sizes and shapes. Nano Lett 7(6): 1542-1550.

32. Connor EE, Mwamuka J, Gole A, Murphy CJ, Wyatt MD (2005) Gold nanoparticles are taken up by human cells but do not cause acute cytotoxicity. Small 1(3): 325-327.

33. Uboldi C, Bonacchi D, Lorenzi G, Hermanns MI, Pohl C, et al. (2009) Gold nanoparticles induce cytotoxicity in the alveolar type-II cell lines A549 and NCIH441. Part Fibre Toxicol 6: 18.

34. de la Fuente JM, Berry CC (2005) Tat peptide as an efficient molecule to trans locate gold nanoparticles into the cell nucleus. Bioconjug Chem 16(5): 1176-1180.

35. Rayavarapu RG, Petersen W, Hartsuiker L, Chin P, Janssen H, et al. (2010) In vitro toxicity studies of polymer-coated gold nanorods. Nanotechnology 21(14): 145101.

36. Takahashi H, Niidome Y, Niidome T, Kaneko K, Kawasaki H, et al. (2006) Modification of gold nanorods using phosphatidylcholine to reduce cytotoxicity. Langmuir 22(1): 2-5.

37. Alkilany AM, Nagaria PK, Hexel CR, Shaw TJ, Murphy CJ, et al. (2009) Cellular uptake and cytotoxicity of gold nanorods: molecular origin of cytotoxicity and surface effects. Small 5(6): 701-708.

38. Huff TB, Hansen MN, Zhao Y, Cheng JX, Wei A (2007) Controlling the cellular uptake of gold nanorods. Langmuir 23(4): 1596-1599.

39. Leonov AP, Zheng J, Clogston JD, Stern ST, Patri AK, et al. (2008) Detoxification of gold nanorods by treatment with polystyrenesulfonate. ACS Nano 2(12): 2481-2488.

40. Parab HJ, Chen HM, Lai TC, Huang JH, Chen PH, et al. (2009) Biosensing, cytotoxicity, and cellular uptake studies of surface-modified gold nanorods. The Journal of Physical Chemistry 113(18): 7574-7578.

**Citation:** Capek I (2015) On Biodecorated Gold Nanoparticles Distributed within Tissues and Cells. J Nanomed Res 2(1): 00020. DOI: 10.15406/jnmr.2015.02.00020

41. Pissuwan D, Valenzuela SM, Killingsworth MC, Xu X, Cortie MB (2007) Targeted Destruction of Murine Macrophage Cells with Bioconjugated Gold Nanorods. J Nanoparticle Res 9(6): 1109-1124.

42. Melancon MP, Lu W, Yang Z, Zhang R, Cheng Z, et al. (2008) In vitro and in vivo targeting of hollow gold nanoshells directed at epidermal growth factor receptor for photothermal ablation therapy. Mol Cancer Ther 7(6): 1730-1739.

43. Pan Y, Neuss S, Leifert A, Fischler M, Wen F, et al. (2007) Size-dependent cytotoxicity of gold nanoparticles. Small 3(11): 1941-1949.

44. Tsoli M, Kuhn H, Brandau W, Esche H, Schmid G (2005) Cellular uptake and toxicity of Au55 clusters. Small 1(8-9): 841-844.

45. Hillyer JF, Albrecht RM (2001) Gastrointestinal per sorption and tissue distribution of differently sized colloidal gold nanoparticles. J Pharm Sci 90(12): 1927-1936.

46. Khlebtsov NG, Dykman LA (2011) Biodistribution and toxicity of gold nanoparticles. Nanotechnologies in Russia 6(1-2): 17-42.

47. Aillona KL, Xiea Y, El-Gendya N, Berklanda CJ, Forresta ML (2009) Effects of nanomaterial physicochemical properties on in vivo toxicit. Adv Drug Deliv Rev 61(6): 457-466.

48. Sadauskas E, Wallin H, Stoltenberg M, Vogel U, Doering P, et al. (2007) Kupffer cells are central in the removal of nanoparticles from the organism. Part Fibre Toxicol 4: 10.

49. Sadauskas E, Danscher G, Stoltenberg M, Vogel U, Larsen A, et al. (2009) Protracted elimination of gold nanoparticles from mouse liver. Nanomedicine 5(2): 162-169.

50. Hillyer JF, Albrecht RM (1998) Correlative Instrumental Neutron Activation Analysis, Light Microscopy, Transmission Electron Microscopy, and X-ray Microanalysis for Qualitative and Quantitative Detection of Colloidal Gold Spheres in Biological Specimens. Microsc Micro anal 4(5): 481-490.

51. Sonavane G, Tomoda K, Makino K (2008) Biodistribution of colloidal gold nanoparticles after intravenous administration: effect of particle size. Colloids Surf B Biointerfaces 66(2): 274-280.

52. Goodman CM, McCusker CD, Yilmaz T, Rotello VM (2004) Toxicity of gold nanoparticles functionalized with cationic and anionic side chains. Bioconjugate Chem 15(4): 897-900.

53. Shukla R, Bansal V, Chaudhary M, Basu A, Bhonde RR, et al. (2005) Biocompatibility of gold nanoparticles and their endocytotic fate inside the cellular compartment: a microscopic overview. Langmuir 21(23): 10644-10654.

54. Gannon CJ, Patra CR, Bhattacharya R, Mukherjee P, Curley SA (2008) Intracellular gold nanoparticles enhance non-invasive radiofrequency thermal destruction of human gastrointestinal cancer cells. J Nanobiotechnology 6: 2.

55. Wang S, Lu W, Tovmachenko O, Rai US, Yu H, et al. (2008) Challenge in understanding size and shape dependent toxicity of gold nanomaterials in human skin keratinocytes. Chem Phys Lett 463(1): 145-149.

56. Chen YS, Hung YC, Liau I, Huang GS (2009) Assessment of the In Vivo Toxicity of Gold Nanoparticles. Nanoscale Res Lett 4(8): 858-864.

57. Pfaller T, Puntes V, Casals E, Duschl A, Oostingh GJ (2009) In vitro investigation of immunomodulatory effects caused by engineered inorganic nanoparticles the impact of experimental design and cell choice. Nanotoxicology 3(1): 46-59.

58. Simon-Deckers A, Brun E, Gouget B, Carriere M, Sicard-Roselli C (2008) Impact of gold nanoparticles combined to X-Ray irradiation on bacteria. Gold Bulletin 41(2): 187-194.

59. Patra HK, Banerjee S, Chaudhuri U, Lahiri P, Dasgupta AK (2007) Cell selective response to gold nanoparticles. Nanomedicine: Nanotechnology. Biology and Medicine 3(2): 111-119.

60. Ikah DSK, Howard CV, McLean WG, Brust M, Tshikhudo TR (2006) Neurotoxic effects of monodispersed colloidal gold nanoparticles. Toxicology 219(1-3): 238.

61. Fan JH, Hung WI, Li WT, Yeh JM (2008) The 13th International Conference on Biomedical Engineering. In: Lim CT & Hong JGC (Eds.), IFMBE Proceedings 23/3. Springer, New York, USA, pp. 870.

62. Singh S, D'Britto V, Prabhune AA, Ramana CV, Dhawan A, et al. (2010) Cytotoxic and Genotoxic Assessment of Glycolipid Reduced and Capped Gold and Silver Nanoparticles. New J Chem 34(2): 294-301.

**Citation:** Capek I (2015) On Biodecorated Gold Nanoparticles Distributed within Tissues and Cells. J Nanomed Res 2(1): 00020. DOI: 10.15406/jnmr.2015.02.00020